References and Notes

1. M. Kulmala *et al.*, *J. Aerosol Sci.* **38**, 289 (2007).
2. C. T. R. Wilson, *Philos. Trans. R. Soc. London Ser. A* **189**, 265 (1897).
3. N. N. Das Gupta, S. K. Ghosh, *Rev. Mod. Phys.* **18**, 225 (1946).
4. H. R. Pruppacher, J. D. Klett, *Microphysics of Clouds and Precipitation* (Kluwer Academic, Dordrecht, Netherlands, 1997).
5. M. Kulmala, L. Pirjola, J. M. Mäkelä, *Nature* **404**, 66 (2000).
6. M. Kulmala *et al.*, *Atmos. Chem. Phys.* **4**, 2553 (2004).
7. M. Kulmala, K. E. J. Lehtinen, A. Laaksonen, *Atmos. Chem. Phys.* **6**, 787 (2006).
8. T. T. Kodas, M. J. Hampden-Smith, *Aerosol Processing of Materials* (Wiley-VCH, New York, 1999).
9. Detailed information on experimental methods, further results, and theory is available as supporting material on *Science* Online.
10. P. E. Wagner, *J. Colloid Interface Sci.* **105**, 456 (1985).
11. P. E. Wagner, D. Kaller, A. Vrtala, A. Lauri, M. Kulmala, *Phys. Rev. E Stat. Nonlin. Soft Matter Phys.* **67**, 021605 (2003).
12. W. Thomson, *Proc. R. Soc. Edinburgh* **7**, 63 (1870).
13. A. B. Nadykto, A. A. Natsheh, F. Yu, K. V. Mikkelsen, J. Ruuskanen, *Phys. Rev. Lett.* **96**, 125701 (2006).
14. N. Fletcher, *J. Chem. Phys.* **29**, 572 (1958).
15. M. Noppel, H. Vehkamäki, M. Kulmala, *J. Chem. Phys.* **119**, 10733 (2003).
16. H. Vehkamäki *et al.*, *J. Chem. Phys.* **126**, 174707 (2007).
17. M. Gamero-Castaño, J. F. de la Mora, *J. Aerosol Sci.* **31**, 757 (2000).
18. M. Kulmala, *Science* **302**, 1000 (2003).
19. M. Kulmala *et al.*, *J. Aerosol Sci.* **35**, 143 (2004).
20. D. Kashchiev, *Nucleation: Basic Theory with Applications* (Butterworth-Heinemann, Oxford, 2000).
21. R. Strey, P. E. Wagner, Y. Viisanen, *J. Phys. Chem.* **98**, 7748 (1994).
22. M. Wilck, F. Stratmann, *J. Aerosol Sci.* **28**, 959 (1997).
23. U. Backman, J. K. Jokiniemi, A. Auvinen, K. E. J. Lehtinen, *J. Nanoparticle Res.* **4**, 325 (2002).
24. P. H. McMurry, *Atmos. Environ.* **34**, 1959 (2000).
25. M. Kulmala, K. E. J. Lehtinen, L. Laakso, G. Mordas, K. Hämeri, *Boreal Environ. Res.* **10**, 79 (2005).
26. T. O. Kim, T. Ishida, M. Adachi, K. Okuyama, J. H. Seinfeld, *Aerosol Sci. Technol.* **29**, 111 (1998).
27. F. Yu, R. P. Turco, *Geophys. Res. Lett.* **27**, 883 (2000).
28. A. A. Lushnikov, M. Kulmala, *Eur. Phys. J. D* **29**, 345 (2004).
29. J. Wedekind, K. Iland, P. E. Wagner, R. Strey, in *Nucleation and Atmospheric Aerosols 2004*, M. Kasahara, M. Kulmala, Eds. (Kyoto Univ. Press, Kyoto, 2004), pp. 49–52.

30. This work was supported by the Austrian Science Foundation (Project No. P16958-N02 and P19546-N20), the Estonian Science Foundation (Grants 6223 and 6988), and the Academy of Finland. The authors declare no competing interests. Authors' contributions statement: experiments (P.M.W. and P.E.W.), nanoparticle generation (G.S., G.P.R., and P.M.W.), data analysis (P.M.W. and A.V.), theory and model calculations (M.K., M.N., H.V., and K.E.J.L.), writing (M.K., P.E.W., P.M.W., G.S., K.E.J.L., M.N., and H.V.).

Supporting Online Material

www.sciencemag.org/cgi/content/full/319/5868/1374/DC1
SOM Text
Figs. S1 to S5
Table S1
References

9 August 2007; accepted 24 January 2008
10.1126/science.1149034

Age and Evolution of the Grand Canyon Revealed by U-Pb Dating of Water Table–Type Speleothems

Victor Polyak,* Carol Hill, Yemane Asmerom

The age and evolution of the Grand Canyon have been subjects of great interest and debate since its discovery. We found that cave mammillaries (water table indicator speleothems) from nine sites in the Grand Canyon showed uranium-lead dating evidence for an old western Grand Canyon on the assumption that groundwater table decline rates are equivalent to incision rates. Samples in the western Grand Canyon yielded apparent water table decline rates of 55 to 123 meters per million years over the past 17 million years, in contrast to eastern Grand Canyon samples that yielded much faster rates (166 to 411 meters per million years). Chronology and inferred incision data indicate that the Grand Canyon evolved via headward erosion from west to east, together with late-stage (~3.7 million years ago) accelerated incision in the eastern block.

Ever since the first geologist known to set eyes on the Grand Canyon, John Strong Newberry in 1858, and the famous John Wesley Powell expedition of 1869 (*1*), the age and origin of the Grand Canyon have remained a subject of great scientific and popular interest. Accurate incision rate data have, until now, come from dating basalt flows and travertine deposits, but these results have not been able to record both the downward and headward incision of the Grand Canyon over its entire history beyond 1 million years ago (Ma) and higher than 100 m above the river (*2*). More than 50 years ago, Arthur Lange, a speleologist, proposed that the study of cave sediments and speleothems (cave formations) could produce an accurate minimum age for the Grand Canyon (*3*). U-series dating of speleothems, and consequently landscape evolution determinations using caves, began in the 1970s by alpha spectrometry (*4*) and were greatly improved by the application of mass spectrometry in the mid-1980s (*5*).

The realization that certain speleothems such as mammillary coatings (Fig. 1) form near groundwater tables [herein referred to as water tables (*6*)], and the fact that many Grand Canyon caves contain mammillary speleothems (*7*), has allowed us to take advantage of advances in U-Pb and U-series analytical techniques in an effort to make the long-sought chronology possible. For the Grand Canyon area (Fig. 2), there is no better niche than caves to find both clastic and chemical sediments that were deposited before, during, and after the incision of the canyon. Equally important, these cave deposits are located throughout the canyon. Caves are not only well suited to contain these deposits, they also provide an ideal environment that preserves and protects them from weathering. These mammillary coatings in the Grand Canyon caves contain sufficient uranium-lead ratios and yield U-Pb dates that place the water table within the canyon at a particular place and at an absolute time. This allows for the incision history of the Grand Canyon to be reconstructed

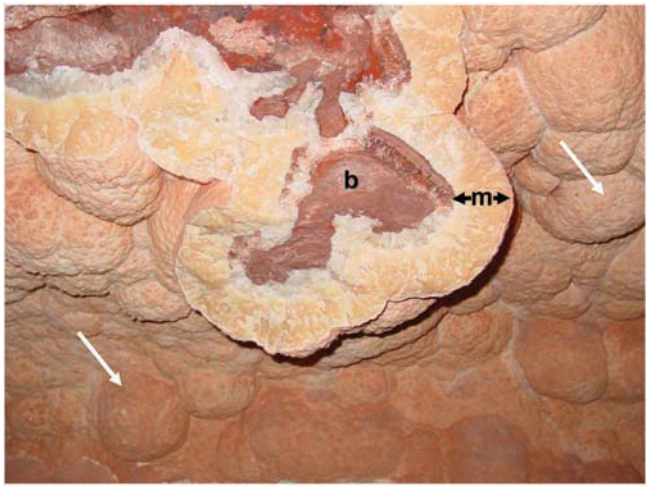

Fig. 1. Cave mammillaries coat cave walls below but near the water table. A cross section of broken mammillaries (m) and exposure of underlying bedrock (b) from site 6 (Tsean Bida) are shown. The unbroken form of this speleothem type (white arrows) indicates a subaqueous origin.

Department of Earth and Planetary Sciences, University of New Mexico, Albuquerque, NM 87131, USA.

*To whom correspondence should be addressed. E-mail: polyak@unm.edu

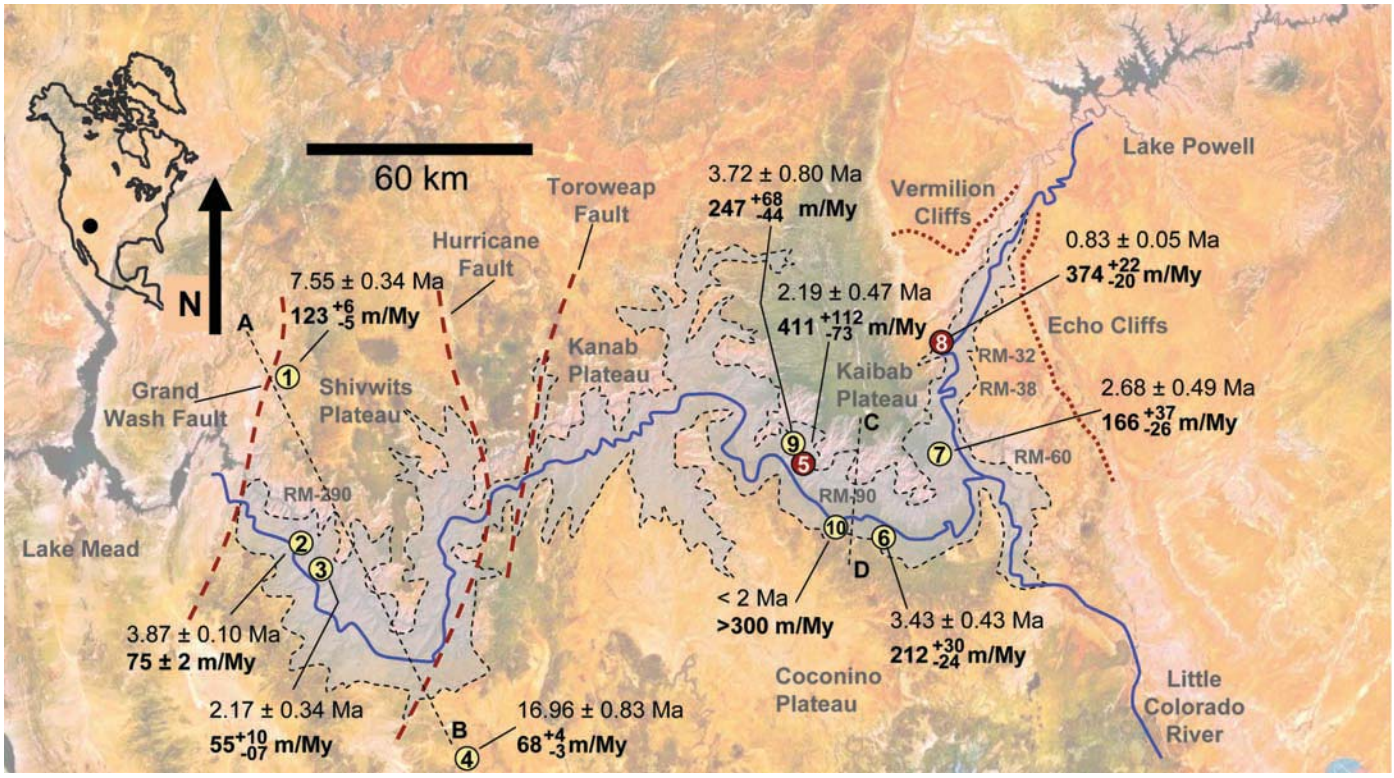

Fig. 2. Map showing locations and U-Pb ages of cave mammillary samples and their apparent incision rates. Site numbers (in circles) are those referred to in Table 1 and the text; those in brown circles represent surface-exposed mammillary calcite. Washout satellite image was taken from the NASA World Wind Web site, with darker regions representing higher elevations. Gray area is the canyon corridor. Two cross sections, A-B and C-D (fig. S3), show generalized pertinent stratigraphy. RM denotes the river-mile location. Incision rate errors assume $\delta^{234}U_{initial}$ values = 3100‰ for sites 1, 2, 4, 6, and 9; see Fig. 3C for expanded uncertainties for these sites.

Table 1. U-Pb ages and incision rates from cave mammillaries. RM, river mile; IR, incision rate. Mother Cave mammillary age is estimated from $\delta^{234}U_{measured}$ of 17 ± 3‰ with $\delta^{234}U_{initial}$ of 3000 ± 2500‰. For sites with $\delta^{234}U_{measured}$ = 0‰, $\delta^{234}U_{initial}$ is assumed to be 3100‰. Extended 2σ absolute errors on the incision rates assume a large uncertainty of the $\delta^{234}U_{initial}$ = 3100 ± 2500‰.

Site	Region	$^{238}U/^{206}Pb$ age (Ma)	$^{235}U/^{207}Pb$ age (Ma)	Concordia-constrained linear 3D age (Ma)	Dist. above river (m)	Dist. from river (km)	RM	IR (m/My)	2σ error	Abs. error	Extended 2σ error	Extended Abs. error
1	Grand Wash Cliffs	7.53 ± 0.42	7.1 ± 1.4	7.55 ± 0.34	930	38.6	277	123	+6	−5	+24	−18
2	Cave B	3.8 ± 0.32	4.3 ± 0.5	3.87 ± 0.10	290	0.5	266	75	+2	−2	+35	−15
3	Dry Canyon	2.17 ± 0.42	8.1 ± 9.9	2.17 ± 0.34	120	1.6	265	55	+10	−7		
4	Grand Canyon Caverns	17.3 ± 1.60	29.0 ± 14.0	16.96 ± 0.83	1160	28.9	190	68	+4	−3	+4	−3
5	Gavain Abyss	2.39 ± 0.77	6.2 ± 5.9	2.19 ± 0.47	900	5.5	93	411	+112	−73		
6	Tsean Bida	3.37 ± 0.50	1.0 ± 16.0	3.43 ± 0.43	726	4.6	80	212	+30	−24	+134	−59
7	Butte Fault Cave	2.73 ± 0.63	3.7 ± 7.9	2.68 ± 0.49	445	2.6	57	166	+37	−26		
8	Bedrock Canyon	0.8 ± 0.12	0.7 ± 0.3	0.83 ± 0.05	310	2.1	32	374	+22	−20		
9	Shinumo Creek Cave	3.5 ± 1.30	−1.0 ± 5.2	3.72 ± 0.80	920	6.6	94	247	+68	−44	+208	−78
10	Mother Cave			^{234}U age = 1.6 ± 0.5	605	2.2	90	>300				

on the basis of the premise that the timing of this water table descent is coeval with incision of the Colorado Plateau by the Colorado River system.

There are three main reasons for placing the deposition of mammillary coatings at or near the water table. First, the fine-grained, fibrous nature of these speleothems attests to the rapid degassing of CO_2 and precipitation of calcite near the water table surface. Second, the Grand Canyon mammillaries are often associated with folia and cave rafts, two speleothem types known to form directly at the water table (*6*). Third, mammillaries can be seen forming near the water table today in caves such as Devils Hole, Nevada (380 km west-northwest of our study area), where they occur along the top few tens of meters of the water table (*8*, *9*). The presence of gypsum rinds in Grand Canyon caves—interpreted to be speleogenetic-type crusts formed by oxidation of H_2S diffusing upward into the caves as the water table drops through the caves (fig. S1)—also supports mammillary association with the water table. These gypsum rinds, which directly overlie mammillary coatings, form just above the water table and display characteristic sulfur isotope ($\delta^{34}S$) values depending on the source of the H_2S (*10*).

Mammillary samples were dated by the U-Pb method (*11*). U-Pb analyses of relatively young carbonate speleothems have recently been shown to be feasible under certain circumstances (*12*), and concerns with excess ^{206}Pb from initial ^{234}U-^{238}U isotopic disequilibrium can be resolved by combining U-Pb data with ^{234}U-^{238}U chronometer data (*12*, *13*): ^{206}Pb data are corrected for ^{234}U excess and ^{230}Th deficiency, and ^{207}Pb data are corrected for ^{231}Pa deficiency (*9*) (fig. S2). Where U-Pb and ^{234}U chronologies overlap, the two systems give consistent chronology.

Our core data (57 analyses) come from nine mammillary coatings throughout the canyon, referred to as sites 1 to 9 (Fig. 2). Four of these coatings (sites 1 to 4) for the western Grand Canyon, all within 1200 vertical meters above the Colorado River, yield ages of 17.0, 7.6, 3.9, and 2.2 Ma. Five other coatings (sites 5 to 9) are located in the eastern Grand Canyon, all within 950 vertical meters above the river, and have ages of 3.7, 3.4, 2.7, 2.2, and 0.8 Ma. For simplicity and consistency, all apparent water table descent rates are based on a relatively flat water table over time. Our U-Pb ages (Table 1 and table S1) show water table descent rates of 55 to 123 m per million years (My) in the western Grand Canyon and 166 to 411 m/My in the eastern Grand Canyon.

Sample sites 1 and 4 are situated 42 and 26 km north and south, respectively, of the Colorado River (Fig. 2) and show water table descent rates that have spatial extent just beyond the canyon itself. Our four western data points support a relatively stable slow drop in the water table in the western Grand Canyon over the past 17 My. In contrast, results from the eastern Grand Canyon show distinctly faster water table descent rates, all having U-Pb ages less than 4 Ma (Fig. 3). In addition, one other site in the eastern Grand Canyon could not be dated by U-Pb (excess common Pb) but has a positive $\delta^{234}U$ value. This sample from Mother Cave near Grand Canyon Village (site 10; Fig. 2 and Table 1) has a ^{234}U-^{238}U age [based on a $\delta^{234}U$ initial value of 3000 ± 2500 per mil (‰)] of 1.6 ± ~0.5, yielding an apparent water table descent rate of >300 m/My; these data provide further evidence of faster eastern Grand Canyon water table descent rates.

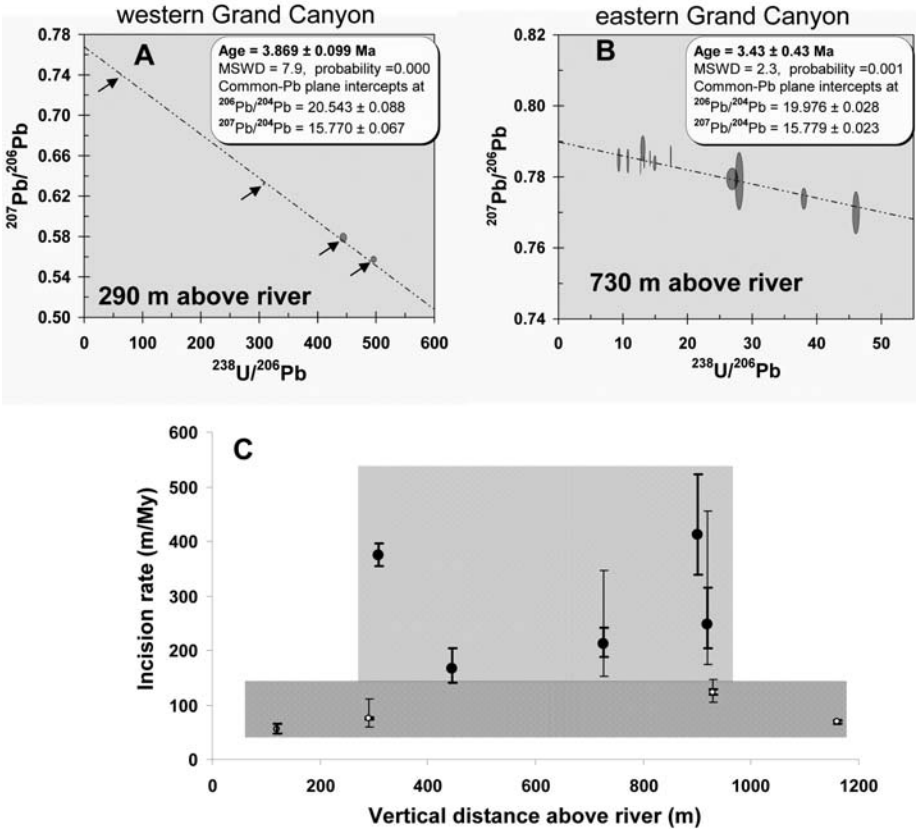

Fig. 3. (**A** and **B**) U-Pb Concordia-constrained linear three-dimensional isochron ages for samples in the western Grand Canyon (A) and the eastern Grand Canyon (B). Note the difference in elevations of these two samples of similar age. These data support a headward erosion scenario for the Grand Canyon. (**C**) Graph illustrating the distinct differences in incision rates in the western versus eastern Grand Canyon. Extended error bars assume a large uncertainty of the $\delta^{234}U_{initial}$ values = 3100 ± 2500‰ for sites 1, 2, 4, 6, and 9.

Western Grand Canyon incision rates are well constrained at 50 to 75 m/My for the last 0.73 My from basalts located within 60 vertical meters above the river (*2*). Our incision rates representing 100 to 1200 m of incision (55 to 75 m/My, excepting site 1) compare well with those determined from the near-river basalt flows and fill an incision rate history gap representing millions of years. Canyon incision by a smaller river system is the most likely interpretation for the relatively stable long-lasting rate of apparent water table descent (55 to 123 m/My) for the western Grand Canyon. This suggests that the western Grand Canyon has been forming for the past 17 My and has probably progressed slowly headward to the east over that entire period. An older western Grand Canyon fits nicely with Miocene extension and timing of Grand Wash fault activity that may represent uplift of the western edge of the Colorado Plateau just prior to 20 Ma (*14*) and filling of the Grand Wash trough with sediment coming from the Virgin Mountains to the north and higher topography just to the east (*15*). A water table descent to the elevation of site 1 (~1200 m above sea level) indicates that erosion of trough sediments was taking place as early as 7.6 Ma. Our incision rate data would imply that Grand Canyon incision into the Grand Wash fault cliffs incised into the top of the Redwall-Muav aquifer of the Colorado Plateau some time between 16 and 9 Ma. Initiation of deposition of the Miocene-aged, lacustrine, Hualapai limestone [11 to 6 Ma (*16*, *17*)] may have been coeval with, and the result of, the release of carbonate-rich water from the newly truncated Redwall Limestone (*14*, *18*).

The eastern third of the Grand Canyon appears to have undergone fast incision (>166 m/My) and rapid headward erosion starting before 3.7 Ma and likely at 5 to 6 Ma when the Colorado River became fully integrated and through-flowing (*17*). A previously reported faster incision rate in the eastern Grand Canyon [150 to 230 m/My for the past 0.5 My; river mile 60 (*19*)] is consistent with our results in that area (140 to 203 m/My) and was compared and attributed to the Hurricane Fault displacement (*2*). However, our data suggest accelerated headward erosion in the eastern Grand Canyon—whether from simple

knick-point propagation, lake overflow (*20*), or karst capture (*18*). Marble Canyon mammillaries also indicate fast incision rates. At river miles 57 (site 7) and 32 (site 8), incision rates are 166 and 374 m/My, respectively, and at river mile 38, a speleogenetic gypsum crust yielded a U-series age of 0.15 Ma at 50 m above the river and an incision rate of ≤330 m/My.

Even though our interpretation assumes no structural or hydrologic complexities, those complexities could help to explain any apparent inconsistencies as data accumulate. However, it is likely that the structure and hydrology will not change the overall interpretation that the western Grand Canyon is older than the eastern Grand Canyon. For instance, an explanation for the higher incision rate at site 1 (Bobcat Cave, Grand Wash Cliffs) could be the presence of an elevated water table north of the western Grand Canyon at 7.6 Ma. Even without this interpretation, the highest western Grand Canyon incision rate from the Grand Wash Cliffs mammillary of 123 m/My (site 1) is still less than the slowest incision rate for the eastern Grand Canyon (166 m/My, site 7; Fig. 3 and fig. S3C). The fast incision rate at Bedrock Canyon (site 8) indicates that 300 m of incision occurred in Marble Canyon over the past 1 My. However, at river miles 57 (site 7) and 60 (*19*), incision rates are slower (~140 to 230 m/My). Structure, hydrology, or headward erosion history (i.e., knick-point propagation from site 7 to site 8) might resolve these differences when additional data are available.

Overall, our data argue for an older Grand Canyon that was modified in the late Miocene by a fully integrated Colorado River that accelerated the headward erosion of the eastern Grand Canyon. We found that mammillary calcite is not restricted to large caves in the Redwall and Muav limestones, but also occurs in small fissure-controlled caves in other units such as the overlying Supai Formation. Hundreds of these deposits probably exist throughout the canyon, offering the potential for a reconstruction of the canyon's history, with a resolution perhaps high enough to explain complexities of the canyon's history related to faults, folds, and volcanic and tectonic activity.

References and Notes

1. W. Ranney, *Carving Grand Canyon—Evidence, Theories, and Mystery* (Grand Canyon Association, Grand Canyon, AZ, 2005).
2. K. E. Karlstrom *et al*., *Geol. Soc. Am. Bull.* **119**, 1283 (2007).
3. A. L. Lange, *Plateau* **27**, 1 (1955).
4. T. C. Atkinson, P. J. Rowe, in *Uranium-Series Disequilibrium: Applications to Earth, Marine, and Environmental Sciences*, M. Ivanovich, R. Harmon, Eds. (Oxford Univ. Press, New York, 1992), pp. 669–703.
5. R. L. Edwards, J. H. Chen, G. J. Wasserburg, *Earth Planet. Sci. Lett.* **81**, 175 (1986).
6. C. A. Hill, P. Forti, *Cave Minerals of the World* (National Speleological Society, Huntsville, AL, 1997).
7. V. J. Polyak, C. A. Hill, Y. Asmeron, *GSA Abs. Prog.* **36**, 549 (2004).
8. I. J. Winograd *et al*., *Science* **242**, 1275 (1992).
9. B. J. Szabo, P. T. Kolisar, A. C. Riggs, I. J. Winograd, K. R. Ludwig, *Quat. Res.* **41**, 56 (1994).
10. C. A. Hill, V. J. Polyak, W. C. McIntosh, P. P. Provencio, in *Colorado River Origin and Evolution*, R. A. Young, E. E. Spamer, Eds. (Grand Canyon Association, Grand Canyon, AZ, 2001), pp. 141–146.
11. See supporting material on *Science* Online.
12. D. A. Richards, S. H. Bottrell, R. A. Cliff, K. Strohle, P. J. Rowe, *Geochim. Cosmochim. Acta* **62**, 3683 (1998).
13. J. Woodhead *et al*., *Quat. Geochronol.* **1**, 208 (2006).
14. J. E. Faulds, L. M. Price, M. A. Wallace, in *Colorado River Origin and Evolution*, R. A. Young, E. E. Spamer, Eds. (Grand Canyon Association, Grand Canyon, AZ, 2001), pp. 93–100.
15. L. S. Beard, *GSA Spec. Pap. 303*, 27 (1996).
16. J. E. Faulds, M. A. Wallace, L. A. Gonzalez, M. T. Heizler, in *Colorado River Origin and Evolution*, R. A. Young, E. E. Spamer, Eds. (Grand Canyon Association, Grand Canyon, AZ, 2001), pp. 81–87.
17. J. E. Spencer, L. Peters, W. C. McIntosh, P. J. Patchett, in *Colorado River Origin and Evolution*, R. A. Young, E. E. Spamer, Eds. (Grand Canyon Association, Grand Canyon, AZ, 2001), pp. 89–92.
18. C. A. Hill, N. Eberz, R. H. Buecher, *Geomorphology* **95**, 316 (2008).
19. J. Pederson, K. Karlstrom, W. Sharp, W. McIntosh, *Geology* **31**, e17 (2003).
20. N. Meek, J. Douglass, in *Colorado River Origin and Evolution*, R. A. Young, E. E. Spamer, Eds. (Grand Canyon Association, Grand Canyon, AZ, 2001), pp. 199–206.

21. Supported by NSF grant EAR-0518602 and by a National Park Service research grant. We thank E. Benenati and K. Voyles for the necessary collection permits; the Navajo, Hopi, and Hualapai tribes for permission to enter and collect from caves on their land; P. Provencio, A. Hill, C. Mosch, and M. Goar for field assistance; S. Davis, D. Powell, M. Oliphant, and N. Pistole for helping us to gain access to remote areas along the river; A. and P. Palmer for help in the field and through cave science discussions along the river; and especially B. and D. Buecher and D. Powell for their tremendous amount of fieldwork and sample elevation-location data.

Supporting Online Material

www.sciencemag.org/cgi/content/full/319/5868/1377/DC1
Materials and Methods
Figs. S1 to S3
Table S1
References

2 October 2007; accepted 30 January 2008
10.1126/science.1151248

The Dust Halo of Saturn's Largest Icy Moon, Rhea

G. H. Jones,[1,2,3*] E. Roussos,[1] N. Krupp,[1] U. Beckmann,[4] A. J. Coates,[2,3] F. Crary,[5] I. Dandouras,[6] V. Dikarev,[1,4,7] M. K. Dougherty,[8] P. Garnier,[6,9] C. J. Hansen,[10] A. R. Hendrix,[10] G. B. Hospodarsky,[11] R. E. Johnson,[12] S. Kempf,[4] K. K. Khurana,[13] S. M. Krimigis,[14,15] H. Krüger,[1] W. S. Kurth,[11] A. Lagg,[1] H. J. McAndrews,[2,19] D. G. Mitchell,[14] C. Paranicas,[14] F. Postberg,[4] C. T. Russell,[13] J. Saur,[16] M. Seiß,[17] F. Spahn,[17] R. Srama,[4] D. F. Strobel,[18] R. Tokar,[19] J.-E. Wahlund,[9] R. J. Wilson,[19] J. Woch,[1] D. Young[5]

Saturn's moon Rhea had been considered massive enough to retain a thin, externally generated atmosphere capable of locally affecting Saturn's magnetosphere. The Cassini spacecraft's in situ observations reveal that energetic electrons are depleted in the moon's vicinity. The absence of a substantial exosphere implies that Rhea's magnetospheric interaction region, rather than being exclusively induced by sputtered gas and its products, likely contains solid material that can absorb magnetospheric particles. Combined observations from several instruments suggest that this material is in the form of grains and boulders up to several decimetres in size and orbits Rhea as an equatorial debris disk. Within this disk may reside denser, discrete rings or arcs of material.

On 26 November 2005, Cassini encountered Rhea, the second largest of Saturn's moons, at 500 km altitude, detecting in situ the anticipated (*1*, *2*), approximately spherical distribution of grains lofted from its surface by interplanetary dust impacts. Cassini passed downstream of Rhea with respect to the local magnetospheric flow (Fig. 1) and observed the anticipated wake caused by plasma striking the moon, together with an unpredicted depletion of energetic electrons extending to ~8 Rhea radii (R_R) (Fig. 2). The scale of the depletion indicates that some material is absorbing electrons within the volume dominated by Rhea's gravitational field: its Hill sphere, of radius 7.7 R_R. Voyager 1 measurements in 1980 previously indicated a broadened depletion's presence farther downstream (*3*). A more distant Cassini flyby in August 2007 also showed evidence of a broad electron depletion (*4*). No such features have yet been observed at Dione and Tethys, but energetic electrons are absorbed by grains ejected from Enceladus's south pole (*5*). The signature's profile indicates that the electron-absorbing material has a near-symmetrical distribution about Rhea. No evidence was found by Cassini's instruments for the presence of large amounts of freshly ionized gas, which could theoretically scatter electrons. Neutral gas and dust populations are therefore the primary absorbing-medium candidates.

As Cassini passed Rhea, its cosmic dust analyzer (CDA) (*6*) registered an increase in the impact rate of >1 μm particles (Fig. 3), signaling the predicted envelopment of the moon (*1*, *2*) by dust ejected by micrometeoroids impacts. An impact-ejecta model (*1*) indicates a